# Crystal Structure of 4-Oxalocrotonate Tautomerase Inactivated by 2-Oxo-3-pentynoate at 2.4 Å Resolution: Analysis and Implications for the Mechanism of Inactivation and Catalysis[†,‡]

Alexander B. Taylor, Robert M. Czerwinski, William H. Johnson, Jr., Christian P. Whitman,* and Marvin L. Hackert*

*Department of Chemistry and Biochemistry and Medicinal Chemistry Division, College of Pharmacy, The University of Texas, Austin, Texas 78712-1071*

*Received July 7, 1998; Revised Manuscript Received August 20, 1998*

ABSTRACT: The crystal structure of 4-oxalocrotonate tautomerase (4-OT) inactivated by the active site-directed irreversible inhibitor 2-oxo-3-pentynoate (2-OP) has been determined to 2.4 Å resolution. The structure of the enzyme covalently modified at Pro-1 by the resulting 2-oxo-3-pentenoate adduct is nearly superimposable on that of the free enzyme and confirms that the active site is located in a hydrophobic region surrounding Pro-1. Both structures can be described as a trimer of dimers where each dimer consists of a four-stranded $\beta$-sheet with two antiparallel $\alpha$-helices on one side. Examination of the structure also reveals noncovalent interactions between the adduct and two residues in the active site. The $\epsilon$ and $\eta$ nitrogens of the guanidinium side chain of Arg-39″ from a neighboring dimer interact respectively with the C-2 carbonyl oxygen and one C-1 carboxylate oxygen of the adduct while the side chain of Arg-61′ from the same dimer as the modified Pro-1 interacts with the C-1 carboxylate group in a bidentate fashion. An additional interaction to the 2-oxo group of the adduct is provided by one of the two ordered water molecules within the active site region. These interactions coupled with the observation that 2-oxo-3-butynoate is a more potent irreversible inhibitor of 4-oxalocrotonate tautomerase than is 2-OP suggest that Arg-39″ and the ordered water molecule polarize the carbonyl group of 2-OP which facilitates a Michael reaction between Pro-1 and the acetylene compound. On the basis of the crystal structure, a mechanism for the enzyme-catalyzed reaction is proposed.

4-Oxalocrotonate tautomerase (4-OT,[1] EC 5.3.2) catalyzes the isomerization of unconjugated $\alpha$-keto acids such as 2-oxo-4-hexenedioate (**1**) to its conjugated isomer, 2-oxo-3-hexenedioate (**3**), through the dienol intermediate 2-hydroxy-2,4-hexadienedioate (**2**) (Scheme 1) (*1*). The enzyme is elaborated by the soil bacterium *Pseudomonas putida mt-2* as part of a degradative pathway that converts various aromatic hydrocarbons to intermediates in the Krebs cycle (*2*). The entire pathway is encoded by the TOL plasmid and enables the bacteria to utilize various aromatic hydrocarbons as their sole sources of carbon and energy.

Scheme 1

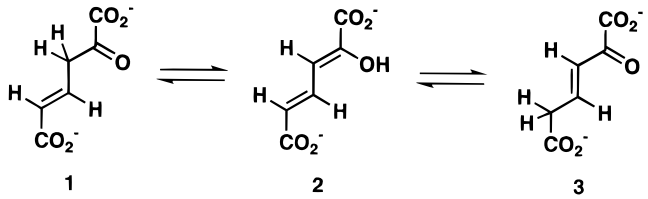


Kinetic and stereochemical studies initially indicated that 4-OT catalyzes a suprafacial 1,3-allylic rearrangement consistent with a one-base mechanism (*3*). Subsequently, Pro-1 was identified as the general base catalyst in the reaction on the basis of affinity labeling studies using 3-bromopyruvate (**4**, 3-BP, Scheme 2) (*4*) and 2-oxo-3-pentynoate (**5**, 2-OP, Scheme 2) (*5*), the chemical synthesis of the cyclopentane-1-4-OT (*6*), and a crystal structure of an isozyme from *Pseudomonas* sp. CF600 strain (*7*). It was further shown by kinetic and NMR studies that Pro-1 has a p$K_a$ of ∼6.4, demonstrating that it can act as a general base under physiological conditions (*8*).

Two arginine residues, Arg-11 and Arg-39, were also implicated in the mechanism because a comparison of the crystal structure of 4-OT to that of the related enzyme 5-(carboxymethyl)-2-hydroxymuconate isomerase (CHMI)

[†] This research was supported by National Institutes of Health Grant GM-41239, the Texas Advanced Research Program (ARP-317), and the Robert A. Welch Foundation (F-1334) to C.P.W. and by National Institutes of Health Grant GM-30105 and the Robert A. Welch Foundation (F-1219) to M.L.H.

[‡] The coordinates have been deposited with the Brookhaven Protein Data Bank (PDB code 1BJP).

* Corresponding authors. M.L.H.: Tel (512)-471-3949; Fax (512)-471-6135; E-mail m.hackert@mail.utexas.edu. C.P.W.: Tel (512)-471-6198; Fax (512)-232-2606; E-mail cwhitman@uts.cc.utexas.edu.

[1] Abbreviations: 3-BP, 3-bromopyruvate; Bu[t], *tert*-butyl; $CDCl_3$, deuterated chloroform; CHMI, 5-(carboxymethyl)-2-hydroxymuconate isomerase; CCM, *cis,cis*-muconate; ESI-MS, electrospray ionization mass spectrometry; $F_o$, and $F_c$, observed and calculated structure factors, respectively; HPLC, high-pressure liquid chromatography; HRMS, high-resolution mass spectrometry; LB, Luria−Bertani medium; NCS, noncrystallographic symmetry; NMR, nuclear magnetic resonance; 2-OB, 2-oxo-3-butynoate; 2-OP, 2-oxo-3-pentynoate; 4-OT, 4-oxalocrotonate tautomerase; RMS, root-mean-square; SDS−PAGE, sodium dodecyl sulfate−polyacrylamide gel electrophoresis; THF, tetrahydrofuran; TFA, trifluoroacetic acid.

10.1021/bi981607j CCC: $15.00 © 1998 American Chemical Society
Published on Web 10/01/1998

Scheme 2

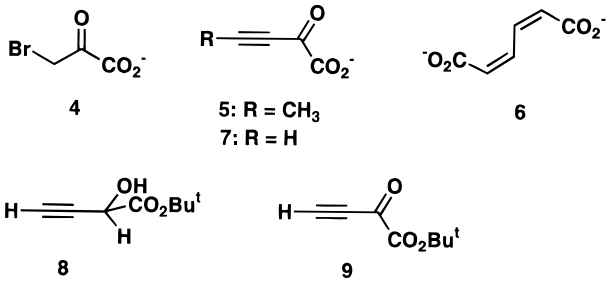


from *Escherichia coli* showed that these two arginines and Pro-1 were among the few conserved residues in the region identified as the active site (*7*). In CHMI, these two arginines are involved in the binding of two sulfate ions which are spaced 6.7 Å apart. This distance is comparable to the distance between the two carboxylate groups of **1** (6.0 Å) and led to the hypothesis that Arg-11 interacts with the 6-carboxylate group while Arg-39 interacts with the C-1 carboxylate group. It was further proposed that Arg-39 functions as a general acid catalyst in addition to its role in binding because there were no other reasonable candidates present in the region. This mechanism assumes that a large conformational change does not occur upon substrate binding (*7*).

The involvement of Arg-11 and Arg-39 in the mechanism was substantiated by NMR studies (*9, 10*). One experiment examined the enzyme covalently bonded to 3-BP, and a second experiment examined the enzyme as a complex with a competitive inhibitor, *cis,cis*-muconate (CCM, **6**) (*9, 10*). The backbone amide chemical shifts for both Arg-11 and Arg-39 change upon the binding of CCM while the interaction of the monocarboxylated 3-BP with enzyme results only in changes for the chemical shifts assigned to Arg-39. These combined observations suggest that the 2-oxo acid portion (C-1 and C-2) of the substrate interacts with Arg-39 while the C-6 carboxylate group interacts with Arg-11.

Although these studies provided experimental evidence consistent with the proposed roles for Arg-11 and Arg-39, they did not explain how Arg-39 could interact with the C-1 carboxylate group and act simultaneously as a general acid catalyst. Attempts to address this question by crystallographic studies of 4-OT complexed with either substrate or 3-BP have not been successful because suitable crystals have not been obtained (*7, 11*). To identify other possible ligands, a number of acetylenic compounds are being synthesized as potential mechanism-based inhibitors of 4-OT. In the course of this work, 2-OP was synthesized and found to be a potent active site-directed irreversible inhibitor (*5*). More significantly, however, crystals of 4-OT inactivated by 2-OP have been obtained.

The crystallization of this complex and the determination of its three-dimensional structure are reported herein. The crystal structure confirms the location of the active site and shows that Pro-1 is attached to C-4 of the species derived from the reaction of 4-OT and 2-OP. The structure also shows that Arg-39″ from a neighboring dimer interacts with the carbonyl oxygen of the 2-oxo group and one oxygen of the C-1 carboxylate group. The active site includes an ordered water molecule which also interacts with the carbonyl oxygen of the 2-oxo group. Moreover, Arg-61′ from the same dimer but from a different monomer as the modified Pro-1 interacts with the C-1 carboxylate group in a bidentate fashion. The nature of the inhibition of 4-OT by 2-OP was further investigated by the synthesis and evaluation of 2-oxo-4-butynoate (**7**, 2-OB, Scheme 2) as an active site-directed irreversible inhibitor. The potency of this compound as an inhibitor suggests that both 2-OP and 2-OB inactivate 4-OT by the Michael addition of Pro-1 to the acetylene compound. The combination of these results provides new insights into the mechanism of inactivation and catalysis.

## EXPERIMENTAL PROCEDURES

### *Materials*

All reagents, buffers, and solvents were obtained from either Aldrich Chemical Co. or Sigma Chemical Co. unless noted otherwise. Tryptone and yeast extract were obtained from Difco (Detroit, MI). The YM-3 ultrafiltration membranes were supplied by Amicon. The syntheses of 2-hydroxy-2,4-hexadienedioate (**2**), *tert*-butyl glyoxylate, and 2-oxo-3-pentynoate (**5**) are described elsewhere (*1, 5*).

### *General Methods*

The mass spectral data for **7** were provided by the mass spectrometry facility at the University of Texas at Austin (Department of Chemistry and Biochemistry). Mass spectra of the modified and unmodified enzyme were obtained on either a Sciex API-III quadrupole electrospray mass spectrometer or a Finnigan MAT LCQ system. NMR spectra were obtained on a Bruker AM-250 spectrometer unless noted otherwise. Chemical shifts were referenced as noted below. The construction of the plasmid pETOT which contains the gene for 4-OT under control of the *phoA* expression system has also been described (*12*). 4-OT was purified according to a literature procedure (*13*). The enzyme was concentrated to ~25 mg/mL in an Amicon filtration cell. Enzyme activity was measured on a Hewlett-Packard 8452A diode array spectrophotometer and monitored by following the formation of **3** at 236 nm (*1*). Protein concentrations were determined by the method of Waddell (*14*).

### *Chemical Syntheses*

*Preparation of tert-Butyl 2-Hydroxy-3-butynoate* (***8***). The synthesis of **8** was carried out under argon following the procedure used for the synthesis of **5** (*5*). To a stirring solution of *tert*-butyl glyoxylate (5.2 g, 40 mmol) in 100 mL of anhydrous THF at −78 °C was added 1-ethynylmagnesium bromide (80 mL, 0.5 M in THF) dropwise over a 30 min period. The product of the reaction was processed as described elsewhere (*5*) to yield **8** as a viscous liquid (2.8 g, 45%): $^1$H NMR ($CDCl_3$, 250 MHz) $\delta$ 1.45 (9 H, s), 2.45 (1 H, d, C-4, $J$ = 5.5 Hz), 4.65 (1 H, d, C-2, $J$ = 5.5 Hz); $^{13}$C NMR ($CDCl_3$, 250 MHz) $\delta$ 27.6 ($CH_3$ of Bu$^t$), 61.4 (C-3), 72.9 (C-2), 79.5 (C-4), 83.8 (C of Bu$^t$), 168.8 (C-1).

*Preparation of tert-Butyl 2-Oxo-3-butynoate (**9**)*. The crude **8** (2.8 g, 17.9 mmol) was oxidized to **9** using lead tetraacetate following the protocol described for the synthesis of **5** (*5*). This procedure generated **9** as a pale yellow liquid (0.24 g, 9%): $^1$H NMR ($CDCl_3$, 250 MHz) $\delta$ 1.53 (9 H, s), 3.55 (1 H, s, C-4); $^{13}$C NMR ($CDCl_3$, 250 MHz) $\delta$ 27.6 ($CH_3$

of Bu$^t$), 79.8 (C-4), 84.6 (C of Bu$^t$), 85.4 (C-3), 157.5 (C-1), 170.4 (C-2).

*Preparation of 2-Oxo-3-butynoic Acid (7).* Hydrolysis of **9** (0.24 g, 1.6 mmol) by anhydrous trifluoroacetic acid (1 mL) following the protocol described for the synthesis of **5** (*5*) generated **7** as a dark yellow solid (0.12 g, 80%): $^1$H NMR (acetone-$d_6$, 250 MHz) $\delta$ 4.55 (1 H, s, C-4), 7.15 (1 H, br s); $^{13}$C NMR (acetone-$d_6$, 250 MHz) $\delta$ 80.8 (C-4), 86.9 (C-3), 160.0 (C-1), 171.7 (C-2); UV (20 mM $NaH_2PO_4$, pH 6.75) $\lambda_{max}$ 224 nm ($\epsilon$ = 3100 $M^{-1}$ $cm^{-1}$); HRMS *m*/*z* calculated for $C_4H_3O_3$ ($MH^+$) 99.0082, found 99.0085.

## *Enzymological Methods*

*Kinetics of Irreversible Inhibition.* The inhibition of 4-OT by **7** was carried out as previously described at 23 °C with the following modifications (*5*). Incubation mixtures (total volume = 1.0 mL) containing varying amounts of **7** (0−8.4 $\mu$M) and enzyme (1.1 $\mu$M) in 20 mM sodium phosphate buffer (pH 6.75) were made up in 1.5 mL Eppendorf micro test tubes. The final pH of the incubation mixtures was 6.90. Aliquots were removed at various time intervals and assayed as described (*5*).

*Protection from Inhibition of 4-OT by 7.* The protection of 4-OT against inactivation by **7** was carried out using an equilibrium mixture of **1**−**3** as described (*5*). 4-OT (1.1 $\mu$M) was incubated with varying concentrations of **2** (0−4.0 mM) in 20 mM sodium phosphate buffer (pH 6.75). After a 5 min interval in which time **2** was converted into an equilibrium mixture of **1**−**3**, a fixed concentration of **7** (8.4 $\mu$M) was added. Aliquots were removed, and the enzyme was assayed for residual activity as described above and elsewhere (*5*).

*Irreversibility of the Inactivation.* The irreversibility of the reaction was established as described previously (*5*) with the following modifications. 4-OT (0.02 $\mu$mol) was incubated with **7** (0.2 $\mu$mol) in 10 mL of 20 mM sodium phosphate buffer (pH 6.8) for 30 min at 4 °C. In a separate control, the same quantity of enzyme was incubated without **7** under identical conditions. Both samples were dialyzed against 20 mM sodium phosphate buffer (pH 6.8) for 39 h. Aliquots (10 $\mu$L) were removed and assayed as described (*5*).

*Mass Spectral Analysis of the Modified 4-OT and Peptide Mapping.* The alkylated residue was identified as previously described with the following modifications (*5*). A quantity of **7** (1.2 mg in 200 $\mu$L of 100 mM $Na_2HPO_4$ buffer, pH 9.2, 12 $\mu$mol) was added to a small volume of 4-OT (2.2 mg, 0.3 $\mu$mol). The addition of **7** to the mixture adjusted the pH to 6.8. The incubation mixture was allowed to incubate at 23 °C for 1 h. There was no residual enzyme activity. A separate control sample made up without **7** was processed identically. Both samples were treated with a solution of $NaBH_4$ (18 mg/200 $\mu$L of $H_2O$) added dropwise and allowed to stand at room temperature overnight. The final pH of the two solutions was ∼7.5. The modified and unmodified 4-OT samples were purified on a Waters system as previously described although they were washed first with $H_2O$/0.05% trifluoroacetic acid for 10 min (*5*). Each purified sample was collected in 2−5 mL (final volume 10 mL) fractions eluting ∼42−43 min after injection. The fractions were analyzed by ESI mass spectrometry. Subsequently, a 3 mL portion of each sample was concentrated to an oily residue and dissolved in ∼1 mL of $H_2O$. After being concentrated again in vacuo, the oily residue was dissolved in 900 $\mu$L of 40 mM ammonium acetate buffer (pH 8), combined with a solution of endoproteinase glu-C (protease V-8) from *Staphylococcus aureus* (12.5 $\mu$g in 100 $\mu$L) dissolved in the same buffer, and treated as previously described (*5*). The peptide fragments were separated and analyzed by ESI-MS on a Finnigan MAT LCQ system using a Wakosil C-18 analytical column. Peptide fragments were eluted by a linear gradient of 0−80% acetonitrile.

## *Structure Determination Methods*

*Crystallization.* 4-OT was cocrystallized in the presence of 2-OP (**5**) using the sitting drop vapor diffusion method. Crystals were grown at 4 °C from 10 $\mu$L drops, which contained 5 $\mu$L of the protein solution (25 mg/mL of 4-OT in 50 mM sodium phosphate buffer at pH 7.4) and 5 $\mu$L of the precipitant solution. The precipitant solution contained 14% poly(ethylene glycol) 8000 in 50 mM sodium phosphate buffer at pH 7.0 and 1 mg of **5** in a total final volume of 500 $\mu$L. The molar ratio of inactivator to protein monomer was 5:1. Crystals first appeared after 24 h and grew to a full size of 0.9 × 0.9 × 0.1 mm in 1 week.

*X-ray Data Collection.* Diffraction data were collected to 2.4 Å resolution from a single crystal of inactivated 4-OT using an RAXIS-IV image plate detector installed on a Rigaku RU200H rotating anode X-ray generator. The generator, equipped with a nickel foil filter, was operated at 5 kW (50 kV × 100 mA). Focusing mirrors were used to produce a collimated beam width of 0.3 mm at the crystal. A sweep of 186° of diffraction data was collected as a set of 124 images of 1.5° oscillations at 25 °C. The exposure time for each image was 6.5 min at a crystal-to-detector distance of 180 mm. The data set is 100% complete to 2.4 Å resolution. All scaling and rejection were performed with DENZO and SCALEPACK (*15*). Analysis of the data suggested a rhombohedral crystal, space group *R*32. The unit cell parameters were $a = b = c = 114.3$ Å and $\alpha = \beta = \gamma = 40.3°$ for the primitive rhombohedral cell. The data were reindexed in the hexagonal setting with unit cell parameters $a = b = 78.7$ Å, $c = 314.6$ Å, $\alpha = \beta = 90°$ and $\gamma = 120°$. A summary of the data collection statistics is listed in Table 1.

*Structure Solution.* The crystal structure of the complexed 4-OT was solved with molecular replacement techniques using a 2.3 Å resolution structure (*R*-factor = 21.6%, $R_{free}^{complete} = 26.8\%$) of the native 4-OT cloned from *P. putida mt-2* as a search model (*11*). The crystal structure of this recombinant 4-OT was solved with molecular replacement techniques using as the search model a 1.9 Å resolution structure of an isozyme of 4-OT from *Pseudomonas* sp. CF600 (PDB entry 1OTF) in which 48 out of 62 amino acids are identical. The Matthews parameter ($V_m$) could not unambiguously predict the number of monomers in the asymmetric unit because the $V_m$ values (3.4−1.7) for 4−8 monomers fall within the range typically observed for globular proteins (*17*). The cross-rotation and translation functions were calculated with AMORE (*18*) using data collected from 10.0 to 4.0 Å resolution. The cross-rotation function gave 16 solutions with correlation coefficients (cc)

Table 1: Crystal and Diffraction Data Collection for the Inactivated 4-OT Complex

| | |
|---|---|
| Crystal Data | |
| space group unit | *R*32 |
| cell dimensions (hexagonal indexing) | |
| *a* (Å) | 78.7 |
| *b* (Å) | 78.7 |
| *c* (Å) | 314.6 |
| Diffraction Data[a] | |
| camera length (mm) | 180 |
| oscillation angle (deg) | 1.5 |
| no. of images | 124 |
| exposure time (min) | 6.5 |
| $R_{meas}$[b] (%) | 15.6 |
| total observations | 248309 |
| unique reflections | 15183 |
| resolution range (Å) | 24.0−2.4 |
| completeness (%) | 100 |
| average $I/\sigma(I)$ | 12.0 |
| redundancy | 9.4 |

[a] Processing of RAXIS−IV image plate data was performed with the *HKL* suite of programs (*15*). [b] $R_{merge}$ corrected for redundancy (*16*).

Table 2: Statistics for the Refined Model of the 4-OT Inactivated Complex[a]

| | |
|---|---|
| resolution range[b] (Å) | 24.0−2.4 |
| no. of reflections used where $F > 2\sigma(F)$ | 14606 |
| no. of protein atoms | 2328 |
| no. of inhibitor atoms | 40 |
| no. of water molecules | 78 |
| deviation in bond distances[c] (Å) | 0. 017 |
| deviation in bond angles[c] (deg) | 1.6 |
| deviation in dihedral angles[c] (deg) | 26.6 |
| deviation in improper torsions[c] (deg) | 0.78 |
| *R*-factor[d] | 0.206 |
| $R_{free}$[d] | 0.244 |

[a] Refinement was performed with the X-PLOR package, version 3.851 (*19*). [b] The bulk solvent correction implemented in the X-PLOR package was applied to the entire resolution range of data used in the refinement (*24*). [c] Root-mean-square deviations from the "ideal" values in the X-PLOR protein_rep.param parameter set. [d] *R*-factor calculations are based on all data with $F > 2\sigma(F)$ including a bulk solvent correction. A test set of 5% of the data was used for the $R_{free}$ calculation (*25*).

ranging from 15.1 to 7.8, using a dimer as the search model. The top solution resulting from the first translation function calculation had a cc of 47.5 and an *R*-factor of 45.6. Two additional translation solutions were found and refined together with the first solution using the rigid body refinement function in AMORE to give a cc of 71.3 and an *R*-factor of 36.7. The asymmetric unit is comprised of five monomers, organized as two dimers and one monomer. The monomer is located at the crystallographic 32 position on the origin that generates one hexamer. The two dimers are aligned along the same crystallographic 3-fold axis that generates two hexamers. The 2-fold axis at the origin produces additional symmetry mates to the two dimers located off the origin. Thus, the primitive rhombohedral unit cell contains five hexamers indicating a $V_m$ ratio (volume/protein mass) of 2.8 Å$^3$/Da (using 6811 as the molecular mass of the 4-OT monomer) and a calculated solvent content of 55%.

*Structure Refinement.* The model for the crystal structure of the inactivated 4-OT complex was refined with computer-based minimization alternated with manual rebuilding using data between 8.0 and 2.4 Å resolution. X-PLOR, version 3.851, was used in all computational refinements (*19*). Manual rebuilding was carried out using $\sigma_A$-weighted $2F_o - F_c$ electron density maps with $F_o - F_c$ maps used to monitor the rebuilding process (*20*). The electron density maps were displayed with the graphics program O (*21*) which was used for model rebuilding. A noncrystallographic symmetry (NCS) matrix was calculated for the five monomers in the asymmetric unit and applied in the initial stages of refinement. Grouped temperature factor refinement, least-squares positional refinement, and simulated annealing were applied to the model (*22*). After the NCS constraints were relaxed by replacing the NCS matrices with energy restraints, the five monomers were modeled individually and designated chains A−E. The inhibitor molecules and three ordered C-terminal residues (residues 60−62) that had not been observed previously in the native structure (*7*) were modeled at this point. The energy parameter files for the inhibitor were created with the XPLO2D program (*23*). The resolution was increased to the full range of 24.0−2.4 Å with a bulk solvent correction (*24*), and individual temperature factor refinement was applied for the remainder of the refinement. Cross-validation methods (*25*) were used to direct refinement progress. Only procedures that decreased $R_{free}$ were used. Solvent molecules were built into the model in the last steps to complete the final model which contains five monomers (two dimers and one monomer), five covalently bound molecules of the adduct derived from 2-OP, and 78 solvent molecules per asymmetric unit. The crystallographic *R*-factor for 14 606 reflections between 24.0 and 2.4 Å resolution is 20.6% ($R_{free}$ is 24.4%). The refinement statistics are summarized in Table 2.

## RESULTS

*Kinetics of Irreversible Inhibition.* The incubation of 4-OT with 2-OB results in the rapid inactivation of the enzyme. The enzyme loses ∼80% of its activity in 4 s when incubated with a stoichiometric excess of inhibitor (10% excess based on the monomer molecular mass of 4-OT). At higher concentrations of inhibitor, there is no detectable enzymatic activity after 4 s. The rapid loss of activity did not permit the collection of sufficiently precise data to assess whether inactivation occurs in a time-dependent first-order fashion. By comparison, the incubation of 4-OT with a stoichiometric amount of 2-OP results in the loss of ∼80% activity in 30 s in a time-dependent first-order fashion (*5*). Binding at the active site of 4-OT by 2-OB is suggested by the observation that an equilibrium mixture of **1**−**3** partially protects the enzyme against rapid inactivation. In the presence of a 4 mM solution of **1**−**3** (total isomer concentration), the enzyme loses only ∼70% of its activity in 30 s even though it is incubated with a 7.7-fold excess of 2-OB. Dialysis (39 h) does not result in any significant reactivation of 4-OT consistent with the formation of a covalent bond between the enzyme and the adduct resulting from 2-OB.

*Identification of the Residue Modified 4-OT by 2-OB.* To obtain further evidence that the inactivation of 4-OT by 2-OB results from the modification of a single residue at the active site and to identify the residue, the enzyme was incubated with 2-OB for 1 h, treated with $NaBH_4$, and purified by reverse-phase HPLC, and the modified enzyme was analyzed by electrospray ionization mass spectrometry (ESI-MS). A sample of 4-OT was treated similarly in the absence of 2-OB.

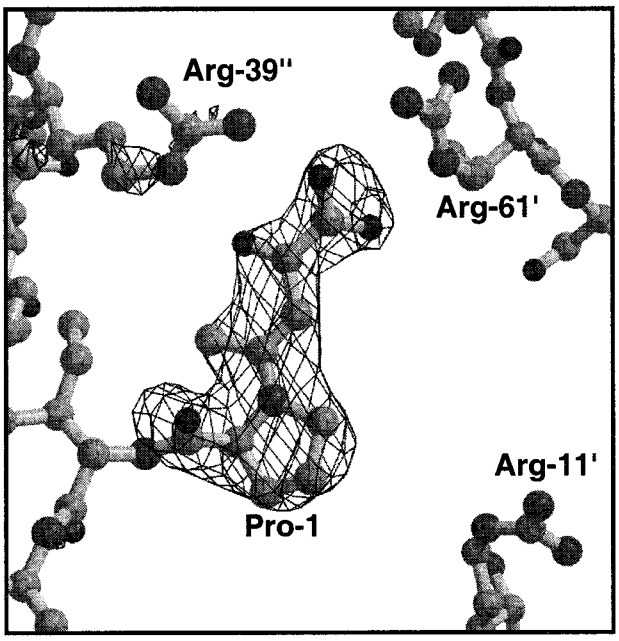


FIGURE 1: $F_o - F_c$ electron density omit map of the covalently bound adduct resulting from the reaction of 4-OT and 2-oxo-3-pentynoate (2-OP). The map was calculated with Pro-1 and the adduct omitted. The adduct interacts with Arg-61′, from the same dimer as the modified Pro-1, and Arg-39″, from the adjacent dimer as described in the text. The map was calculated at 2.4 Å resolution and contoured at 3.0$\sigma$. The figure was prepared with the programs BOBSCRIPT (*33*) and RASTER3D (*34*).

ESI-MS analysis of the untreated 4-OT showed a molecular mass of 6810.4 Da which is in excellent agreement with the expected subunit molecular mass of 6810.7 (average isotopic composition) (*6*). ESI-MS analysis of the inactivated and reduced 4-OT showed a molecular mass of 6912.1 Da. The difference between these masses is 101.7 Da, which indicates that the mass of the bound species is 102.7 Da.

The site of the single modification was identified by subjecting the inactivated, reduced, and purified 4-OT to proteolytic digestion by endoproteinase glu-C (protease V-8) and separating the resulting peptides by HPLC. The HPLC chromatogram shows three well-defined peaks with retention times of approximately 8.7, 10.6, and 11.6 min. Analysis of these peaks by ESI-MS revealed that each peak consisted of several components. A mass (1135.6 Da) corresponding to the modified amino-terminal fragment $C_4H_7O_3$-Pro-1 to Glu-9 (PIAQIHILE) was found near the beginning of the peak eluting at 10.6 min. This fragment was not found in the peptide mixture resulting from proteolytic digestion of the unmodified 4-OT. These results indicate that a single site on the enzyme has been modified which is located on the nine-residue amino-terminal fragment. The only chemically reasonable sites for alkylation within this fragment are Pro-1 and His-6. Because His-6 is not in the active site, and 2-OB is an active site-directed irreversible inhibitor, it can be concluded that Pro-1 is the alkylated residue.[2]

*Structure Determination and Quality.* The structure of 4-OT inactivated by 2-OP has been solved using molecular replacement techniques and refined against 2.4 Å resolution data to a crystallographic *R*-factor of 20.6% and an $R_{free}$ = 24.4%. The electron density for the polypeptide backbone was continuous and well-defined for all residues in three of the five monomers in the asymmetric unit. The remaining two monomers showed only weak or no electron density for the three C-terminal residues (for one monomer) and the four C-terminal residues (for the other monomer). In both $2F_o - F_c$ and $F_o - F_c$ maps, strong electron density in an otherwise flat map is found for the inhibitor in the region previously suggested to be the active site (Figure 1) (*7*). The free hexameric structure of an isozyme of 4-OT from *Pseudomonas* sp. CF600 strain has previously been described as a trimer of dimers with molecular 32 symmetry (*7*). The monomer and dimer of the inactivated 4-OT complex are shown in ribbon diagrams in panels A and B of Figure 2, respectively. The crystallographic asymmetric unit consists of five 4-OT monomers designated chains A−E. The AB dimer contains residues 1−62 for each monomer. The CD dimer contains residues 1−58 and residues 1−60, from chains C and D, respectively. Chain E, the monomer located at the crystallographic 32 position, contains residues 1−62.

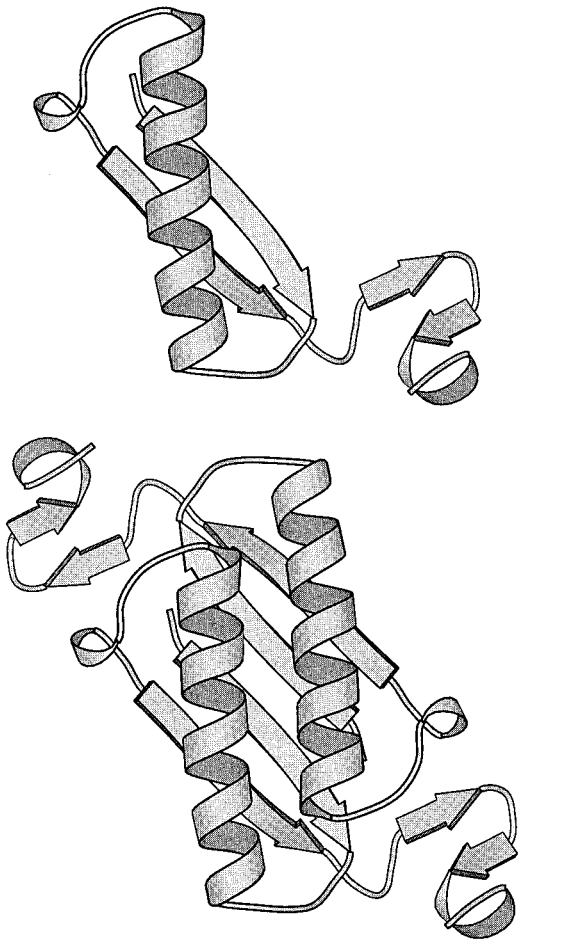

FIGURE 2: Ribbon diagrams showing the monomer and dimer of 4-OT modified by the 2-oxo-3-pentenoate adduct. (A, top) The modified 4-OT monomer consists of two parallel $\beta$-strands, one $3_{10}$ helix, one α-helix, and a single-turn α-helix at the C-terminus. (B, bottom) The modified 4-OT dimer consists of a four-stranded $\beta$-sheet with two antiparallel α-helices on one side and the single-turn α-helices at the C-termini. The figures were prepared with the program MOLSCRIPT (*35*).

[2] Two observations rule out the modification of the side chains of either Gln-4 or Glu-9. It is unlikely that either is sufficiently nucleophilic to react with 2-OB in a Michael reaction, and the crystal structure of 4-OT modified by the homologous compound, 2-OP, clearly shows that Pro-1 is alkylated.

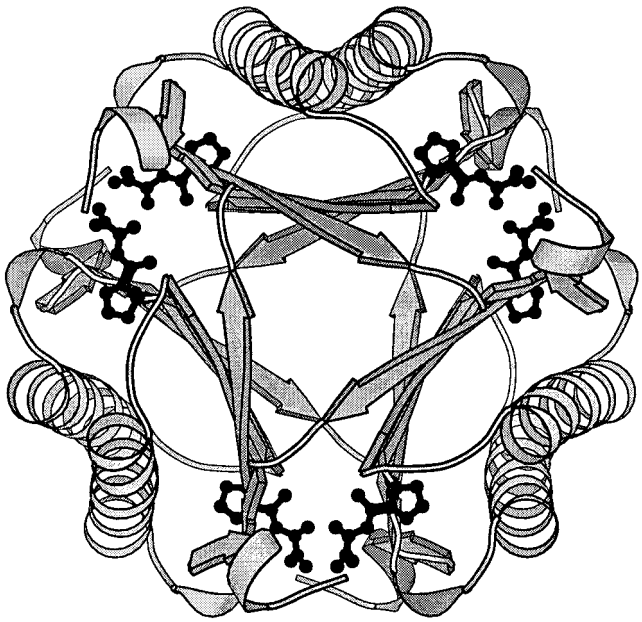

FIGURE 3: 4-OT hexamer viewed down the molecular 3-fold axis showing the modified amino-terminal prolines and confirming the location of the six active sites. Each adduct is stabilized by interactions from neighboring dimers, suggesting that each active site is made up of residues from adjacent dimers.

A Ramachandran plot [calculated with PROCHECK (*26*)] for the $\phi$, $\varphi$ angles shows that all non-glycine and non-proline residues fall within either the most favored regions (96.2%) or additionally allowed regions (3.8%) of low conformational energy. The mean temperature factors between a single dimer and the remainder of the asymmetric unit differ significantly. Chains A, B, and E have mean temperature factors of 19.7, 21.6, and 20.0, respectively, compared to 34.2 and 36.8 for chains C and D. Although the structures of the five monomers do not exhibit significant differences, the difference in temperature factors may be indicative of a different flexibility of the hexamer comprised of chains C and D within the crystal. The C-terminal residues for the dimer composed of chains C and D are not traceable, most likely due to a combination of factors: the CD dimer has a higher overall *B*-factor compared to the rest of the asymmetric unit and the C-terminal region has high *B*-factors compared to the rest of the monomer observed in the native structure. The three C-terminal residues of the free structure are disordered, suggesting flexibility and disorder in this region of the inactivated enzyme structure (*7, 11*). The average RMS difference of $C_\alpha$ positions between monomers is 0.16 Å for chains B−E aligned with chain A.

*Topology of the Free and 4-OT Complex Structures*. In the two previously described free crystal structures of 4-OT [from *Pseudomonas* sp. CF600 (*7*) and from *P. putida mt-2* (*11*)], each monomer consists of a two-stranded parallel $\beta$-sheet linked by a right-handed crossover containing an $\alpha$-helix and a $3_{10}$ helix, followed by a $\beta$-hairpin turn near the C-terminus. Dimerization leads to a four-stranded $\beta$-sheet with antiparallel $\alpha$-helices on one side of the sheet, exemplifying the $\alpha/\beta$ sandwich motif (*7*). The hexamer is stabilized by interactions of a strand from the $\beta$-hairpin turn and one side of the four-stranded sheet between dimers. In summary, the structure of the 4-OT hexamer has a hydrophobic core formed by three, four-stranded $\beta$-sheets surrounded by three sets of $\alpha$-helix pairs.

Scheme 3

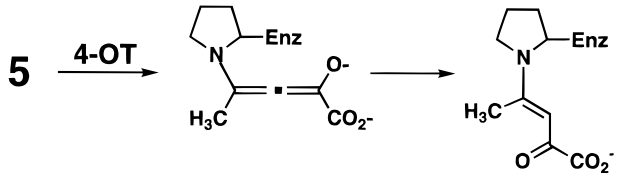


The crystal structures of free 4-OT and 4-OT covalently modified at Pro-1 by its incubation with 2-OP show that the overall folds and structures are comparable even though the free and complexed enzymes crystallize in different space groups. The free enzyme from *Pseudomonas* sp. CF600 crystallized in the space group *P*1 (*7*) while the enzyme from *P. putida mt-2* has been crystallized in the space groups $P2_12_12_1$ (*27*), *R*3, and *P*321 (*11*). The inactivated enzyme crystallizes in a previously unobserved space group *R*32. The single major difference between the free and the inactivated enzyme structures is that covalent modification of 4-OT results in a single-turn $\alpha$-helix at the C-terminus where the residues in this region were previously unobservable in the native structure from *Pseudomonas* sp. CF600.

*Substrate/Inhibitor Binding Site.* The substrate binding pocket of 4-OT was previously identified as a cavity on the surface of the enzyme at one end of two $\beta$-strands primarily because it was in a similar location to the sulfate binding pocket of CHMI (*7*). An electrostatic surface potential map calculated in GRASP (*28*) indicated a pair of positively charged binding pockets due to the presence of several arginines previously implicated as active site residues (*7*). The positively charged pocket was anticipated to accommodate the negatively charged dicarboxylated substrate.

The covalently bound adduct derived from 2-OP confirms the location of the active site at Pro-1. The structure also shows that all six active sites within a hexamer are modified.[3] Unexpectedly, however, the adduct interacts with residues from two adjacent dimers and not just from residues within a single dimer (Figure 3). There are also two ordered water molecules that are conserved in the active site regions of both the free and the complexed 4-OT. One water molecule is positioned between the nitrogen of Pro-1 and the backbone amide hydrogen of Leu-8′. It binds in the region where the C-6 group of substrate is anticipated to bind, and it may be displaced upon substrate binding.

*Interaction of the Adduct with Active Site Residues of 4-OT.* One proposed mechanism for the inactivation of 4-OT involves the Michael addition of Pro-1 to C-4 of 2-OP as shown in Scheme 3 (*5*). Tautomerization of the enol (or enolate) intermediate generates 4-OT modified at Pro-1 by a 2-oxo-3-pentenoate adduct. The crystal structure of the

[3] In contrast, mass spectral analysis of the enzyme treated with either 2-OP or 2-OB and reduced by $NaBH_4$ shows that a significant portion (>50%) of the enzyme is not modified (*5*). Mass spectral analysis of the enzyme modified by 3-BP and reduced by $NaBH_4$ shows that nearly all of the enzyme is modified (*4*). These discrepancies can be explained by the observation that the adduct derived from either acetylene compound can readily form an enamine while that derived from 3-BP cannot. Assuming that nearly all of the enzyme is initially modified by either 2-OP (as shown by the crystal structure) or 2-OB, then the observed final mixture of unmodified and modified enzyme may result from the competing reactions (hydrolysis vs reduction) that the enamine can undergo in the presence of $NaBH_4$.

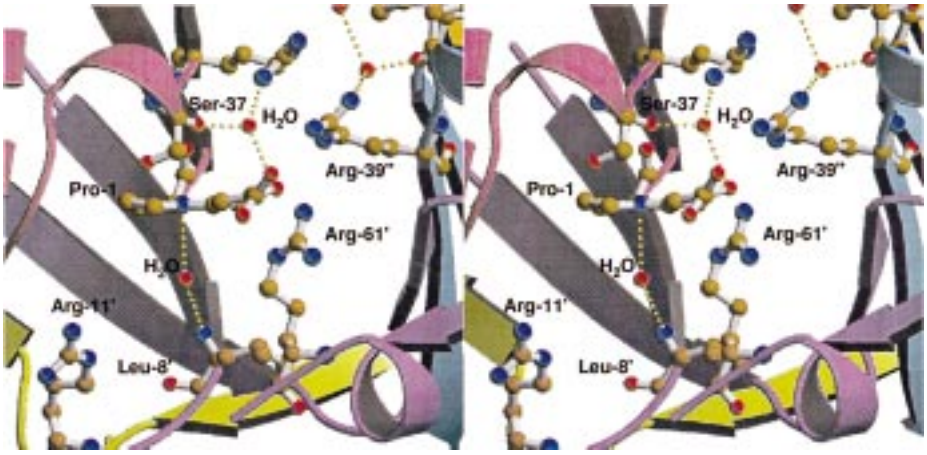


FIGURE 4: Stereo diagrams of an active site of 4-OT. The adduct interacts with active site residues contributed from three monomers. Pro-1, Arg-11′, and Arg-61′ are located in one dimer while Arg-39″ is located in a neighboring dimer. An ordered water molecule also interacts with the carbonyl oxygen of the adduct.

inactivated complex obtained by the incubation of 4-OT and 2-OP shows several key interactions between this adduct and residues in the active site region (Figure 4). First, the structure confirms the presence of a covalent bond between C-4 of the adduct and Pro-1, consistent with the mechanistic proposal for inactivation. The structure also shows that the enzyme-bound adduct has the *E* configuration about the C-3, C-4 bond (Scheme 3). The carbonyl oxygen of the adduct is within 2.9 Å of the side chain $\epsilon$-nitrogen of Arg-39″ from the neighboring dimer. Arg-39″ also provides an additional interaction from its side chain $\eta$-nitrogen to one carboxylate oxygen of the adduct as the distance between them is 2.7 Å. The same carboxylate oxygen is within 3.2 Å of the side chain $\eta$-nitrogen of Arg-61′. The other carboxylate oxygen of the adduct is within 3.0 Å of the side chain $\epsilon$-nitrogen of Arg-61′. The C-5 methyl group of the adduct is situated in a hydrophobic pocket consisting primarily of the side chains of Ile-2, Met-45′, and Phe-50′. The adduct also interacts with one of the two conserved water molecules. In the free enzyme, this water molecule forms a hydrogen bond with the backbone carbonyl oxygen of Ser-37. In the complexed enzyme structure, this water molecule forms additional hydrogen bonds with the C-2 keto group of the covalently bound adduct and a terminal amino group of Arg-39″. The distance between the carbonyl oxygen and the water molecule is 3.1 Å.

The crystal structure indicates that the adduct interacts with residues from two adjacent dimers (Figure 5). Thus, the modified Pro-1 is contained within one dimer, and Arg-39″ is from the neighboring dimer. Arg-61′ is within the same dimer as the modified Pro-1 but from the other monomer. This arrangement suggests that residues of potential catalytic importance come from adjacent dimers and not just from within the same dimer.

A further implication of this observation is that two active sites (from adjacent dimers) are significantly close to each other. The C-1 carboxylate groups of two bound adducts are separated by a distance of 10.7 Å and the guanidinium groups of two intervening Arg-39 residues. Despite the proximity of two active sites, it appears that a substrate molecule can be bound at each site simultaneously, which is consistent with the experimental finding that cooperativity is not observed for the substrate.

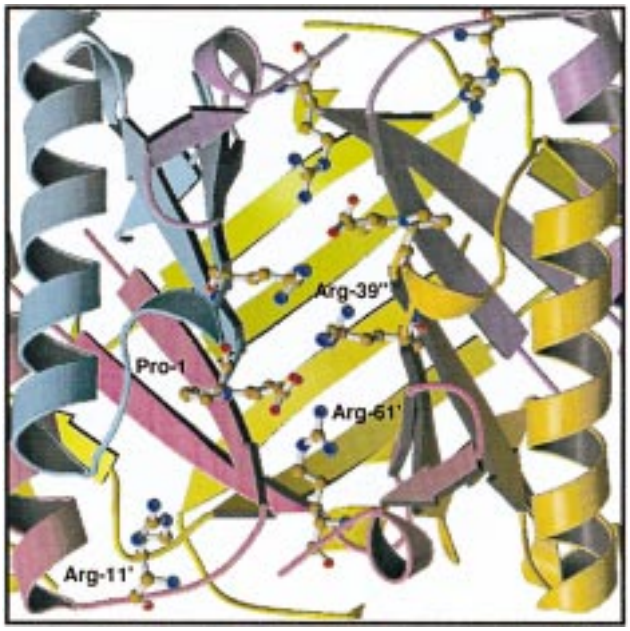


FIGURE 5: Ribbon diagram showing the relative locations of two active sites at the interface of adjacent dimers. The residues of the lower active site are labeled. Both amino-terminal prolines are modified as shown. The ordered water molecule is not shown.

## DISCUSSION

The inactivation of 4-OT by 2-OP has been studied previously and partially characterized (*5*). Two mechanisms were proposed to account for the inactivation of 4-OT by 2-OP. The first involves a Michael reaction in which Pro-1 attacks the C-4 position of 2-OP as shown in Scheme 3. A second mechanism involves the enzyme-catalyzed allylic rearrangement of 2-OP to the allene **10** (Scheme 4). Pro-1 can then react at C-4, resulting in covalent modification of the enzyme. The position of the double bond will be determined by whether protonation occurs at C-3 or C-5. In the first mechanism, 2-OP acts as an active site-directed irreversible inhibitor while in the second mechanism 2-OP acts as a mechanism-based inhibitor.

The kinetic studies using 2-oxo-3-butynoate (**7**) indicate that it is a more potent inhibitor than 2-OP. Because 2-OB lacks the C-5 methyl group, it cannot undergo rearrangement to the allene so that the inactivation of 4-OT can only occur

Scheme 4

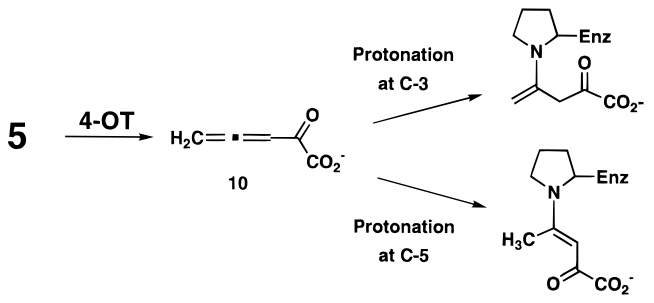


by a Michael reaction. This observation suggests that the structurally homologous 2-OP is sufficiently reactive to alkylate Pro-1 in a Michael reaction. Presumably, the electron-donating effect and/or the steric effect of the C-5 methyl group make 2-OP less reactive than 2-OB. The greater reactivity of 2-OB raises a concern about its specificity and whether it inactivates 4-OT by the modification of Pro-1 or by the modification of one or more residues not involved in catalysis. Three lines of evidence clearly demonstrate that 2-OB reacts at the active site and modifies Pro-1. First, the enzyme is partially protected from inactivation by the presence of substrate. Second, mass spectral analysis shows that only one residue per monomer is modified by 2-OB. Finally, the site of modification is found on the same nine-residue amino-terminal fragment, Pro-1 to Glu-9, determined to be the location of the site of modification for 2-OP.

The crystal structure of 4-OT inactivated by 2-OP validates the previous chemical and kinetic experiments characterizing the reaction and identifies the probable interactions at the active site leading to the alkylation of Pro-1. As noted above, a single site on the enzyme is modified by the adduct derived from 2-OP which is localized to the amino-terminal fragment Pro-1 to Glu-9 (*5*). The crystal structure of the inactivated enzyme confirms that Pro-1 is the modified residue and shows that 2-OP binds at the active site and irreversibly inhibits the enzyme by the formation of a covalent bond. The crystal structure also shows that the adduct derived from 2-OP interacts with an ordered water molecule (at the carbonyl oxygen at C-2) as well as the side chains of Arg-61′ (at the C-1 carboxylate group), Arg-39″ (at one carboxylate oxygen of C-1 and the carbonyl oxygen at C-2), and Ile-2, Met-45′, and Phe-50′ (the C-5 methyl group). Because Arg-39″ and the water molecule interact with the C-2 carbonyl oxygen of the adduct, it can be inferred that they polarize the C-2 carbonyl group of 2-OP and stabilize the intermediate (shown as an enolate in Schemes 3 and 5). This may be analogous to the stabilization of the transition state provided by the oxyanion hole in serine protease-catalyzed reactions (*29*). Polarization of the carbonyl group would facilitate a Michael reaction between 2-OP and 4-OT and lead to inactivation.

One further implication of this mechanism is that residues from adjacent dimers are involved in the inactivation process. This observation provides an alternate explanation for the half-site stoichiometry previously reported for the inactivation of 4-OT by 3-bromopyruvate. This phenomenon was proposed to result from an intradimer conformational change in which the modification of one monomer disrupted the second active site within the same dimer (*4*). This mechanism was based on the crystal structure of the free enzyme which suggested that each dimer consisted of two active sites made up of residues from both monomers (*7*). The crystal structure of the inactivated complex, in which the modified adduct interacts with residues from two neighboring dimers, suggests that the observed half-site stoichiometry results from an interdimer conformational change. Thus, the modification of Pro-1 in one dimer may slow or preclude the modification of the neighboring dimer.

If the interactions observed in the inactivated complex can be extrapolated to the enzyme-catalyzed isomerization of **1** to **3**, then the mechanism shown in Scheme 5 can be proposed, in which the intermediate **2**, shown as the dienolate, is stabilized by similar interactions. There is some justification for such an extrapolation because the active sites of the free enzyme and the inactivated enzyme are identical in many respects, indicating that the formation of the covalent bond has not grossly distorted the active site. Thus, as shown in Scheme 5, the dienolate intermediate may be stabilized by two hydrogen bonds, one from the ordered water molecule and a second one from the side chain of Arg-39″. The C-1 carboxylate group of **2** may be involved in a bidentate interaction with the side chain of Arg-61′. There may be an additional interaction between the C-1 carboxylate group of **2** and the guanidinium group of Arg-39″.

This arrangement, if it does indeed accurately portray the stabilization of the reaction intermediate, has three implications for catalysis by 4-OT. First, the presence of Arg-61′ implies that a conformational change takes place upon substrate binding which moves Arg-61′ into the active site. Such a conformational change is consistent with the fact that the most notable difference between the structures of the free and the inactivated enzymes is that the three C-terminal

Scheme 5

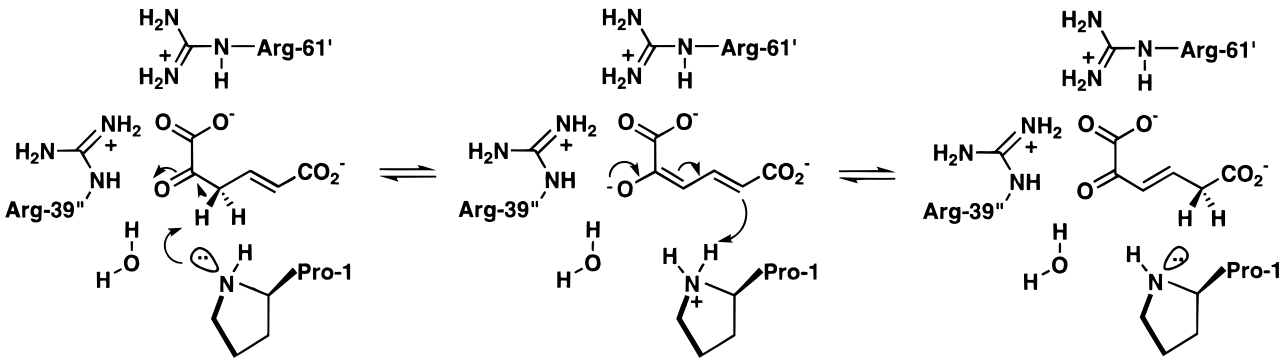

residues are observable in the structure of the inactivated enzyme. Second, the involvement of Arg-39″ from the adjacent dimer suggests that the active site of 4-OT is at the interface of two dimers, indicating that the hexameric structure is required for enzymatic activity. Presumably, there are two active sites at each interface consisting of residues from the adjacent dimers. Finally, the catalytic strategy used by 4-OT for the isomerization of **1** to **3** appears to be somewhat more complex than previously thought (*4*, *7*, *8*). As noted at the outset, Pro-1 and Arg-39 have been identified respectively as the general base and general acid catalysts. The working hypothesis for the mechanism involved the abstraction of the C-3 proton of **1** by Pro-1 to generate the dienolate intermediate, **2**. The reaction intermediate was presumably stabilized by Arg-39 (from the same dimer) acting as a general acid catalyst (*4*, *7*, *8*). The newly postulated role for the ordered water molecule in the inactivation mechanism suggests that it and Arg-39″ are responsible for the stabilization of **2** in that each may provide a hydrogen bond to the oxyanion (Scheme 5). A somewhat analogous situation has been proposed for the $\Delta^5$-3-ketosteroid isomerase-catalyzed reaction (*30*−*32*). Recent crystallographic and NMR studies show that a dienolate reaction intermediate is stabilized by two hydrogen bonds—one hydrogen bond is provided by Tyr-14 and a second hydrogen bond is provided by Asp-99. Further analysis indicated that Tyr-14 forms a stronger hydrogen bond to the reaction intermediate. The strength of the two proposed hydrogen bonds utilized to stabilize the reaction intermediate in the 4-OT reaction is not yet known. Moreover, it is possible that Arg-39″ stabilizes the reaction intermediate by an electrostatic interaction and not by a hydrogen bond. These and other questions raised by the crystal structure of the inactivated complex are currently being investigated.

## ACKNOWLEDGMENT

We gratefully acknowledge Dr. Michael C. Fitzgerald (Scripps Research Institute, La Jolla, CA) and Dr. Moini Mehdi (Department of Chemistry and Biochemistry, University of Texas, Austin, TX) for their acquisition and analysis of several mass spectra. We also thank David Lola for his assistance in the proteolytic digestion of the unmodified and modified samples of 4-OT.

## REFERENCES

1. Whitman, C. P., Aird, B. A., Gillespie, W. R., and Stolowich, N. J. (1991) *J. Am. Chem. Soc. 113*, 3154−3162.
2. Harayama, S., Rekik, M., Ngai K.-L., and Ornston, L. N. (1989) *J. Bacteriol. 171*, 6251−6258.
3. Lian, H., and Whitman, C. P. (1993) *J. Am. Chem. Soc. 115*, 7978−7984.
4. Stivers, J. T., Abeygunawardana, C., Mildvan, A. S., Hajipour, G., Whitman, C. P., and Chen, L. H. (1996) *Biochemistry 35*, 803−813.
5. Johnson, W. H., Jr.; Czerwinski, R. M., Fitzgerald, M. C., and Whitman, C. P. (1997) *Biochemistry 36*, 15724−15732.
6. Fitzgerald, M. C., Chernushevich, I., Standing, K. G., Whitman, C. P., and Kent, S. B. H. (1996) *Proc. Natl. Acad. Sci. U.S.A. 93*, 6851−6856.
7. Subramanya, H. S., Roper, D. I., Dauter, Z., Dodson, E. J., Davies, G. J., Wilson, K. S., and Wigley, D. B. (1996) *Biochemistry 35*, 792−802.
8. Stivers, J. T., Abeygunawardana, C., Mildvan, A. S., Hajipour, G., and Whitman, C. P. (1996) *Biochemistry 35*, 814−823.
9. Stivers, J. T., Abeygunawardana, C., Whitman, C. P., and Mildvan, A. S. (1996) *Protein Sci. 5*, 729−741.
10. Stivers, J. T., Abeygunawardana, C., Mildvan, A. S., and Whitman, C. P. (1996) *Biochemistry 35*, 16036−16047.
11. Taylor, A. B. (1998) Ph.D. Dissertation, University of Texas, Austin, TX.
12. Chen, L. H., Kenyon, G. L., Curtin, F., Harayama, S., Bembenek, M. E., Hajipour, G., and Whitman, C. P. (1992) *J. Biol. Chem. 267*, 17716−17721.
13. Czerwinski, R. M., Johnson, W. H., Jr., Whitman, C. P., Harris, T. K., Abeygunawardana, C., and Mildvan, A. S. (1997) *Biochemistry 36*, 14551−14560.
14. Waddell, W. J. (1956) *J. Lab. Clin. Med. 48*, 311−314.
15. Otwinowski, Z., and Minor, W. (1996) *Methods Enzymol. 276*, 307−326.
16. Diederichs, K., and Karplus, P. A. (1997) *Nat. Struct. Biol. 4*, 269−275.
17. Matthews, B. W. (1968) *J. Mol. Biol. 33*, 491−497.
18. Navaza, J. (1994) *Acta Crystallogr. A50*, 157−163.
19. Brunger, A. T., Kuriyan, J., and Karplus, M. (1987) *Science 235*, 458−460.
20. Read, R. J. (1986) *Acta Crystallogr. A42*, 140−149.
21. Jones, A. T., Zou, J. T., Cowan, S. W., and Kjeldgaard, M. (1991) *Acta Crystallogr. A47*, 110−119.
22. Brunger, A. T., Krukowski, A., and Erickson, J. (1990) *Acta Crystallogr. A46*, 585−593.
23. Kleywegt, G. J. (1995) *CCP4/ESF-EACBM Newsl. Protein Crystallogr. 31*, 45−50.
24. Jiang, J.-S., and Brunger, A. T. (1994) *J. Mol. Biol. 243*, 100−115.
25. Brunger, A. T. (1992) *Nature 355*, 472−474.
26. Laskowski, R. A., MacArthur, M. W., Moss, S. D., and Thornton, J. M. (1993) *J. Appl. Crystallogr. 26*, 283−291.
27. Davenport, R. C., and Whitman, C. P. (1993) *J. Mol. Biol. 231*, 509−512.
28. Nicholls, A., and Honig, B. (1991) *J. Comput. Chem. 12*, 435−445.
29. Kraut, J. (1977) *Annu. Rev. Biochem. 46*, 331−358.
30. Wu, Z. R., Ebrahimian, S., Zawrotny, M. E., Thornburg, L. D., Perez-Alvarado, G. C., Brothers, P., Pollack, R. M., and Summers, M. F. (1997) *Science 276*, 415−417.
31. Kim, S. W., Cha, S.-S., Cho, H.-S., Kim, J.-S., Ha, N.-C., Cho, M.-J., Joo, S., Kim, K. K., Choi, K. Y., and Oh, B.-H. (1997) *Biochemistry 36*, 14030−14036.
32. Cho, H.-S., Choi, G., Choi, K. Y., and Oh, B.-H. (1998) *Biochemistry 37*, 8325−8330.
33. Esnouf, R. M. (1997) *J. Mol. Graphics 15*, 132−134.
34. Merritt, E. A., and Bacon, D. J. (1997) *Methods Enzymol. 277*, 505−524.
35. Kraulis, P. J. (1991) *J. Appl. Crystallogr. 24*, 946−950.

BI981607J